Understanding the activity of Zn-Cu sites in methanol synthesis

Batyrev, E.D.

Publication date
2013

Chapter 2

The effect of the reduction temperature on the structure of $Cu/ZnO/SiO_2$ catalysts for methanol synthesis*

Abstract

The structure of Cu/SiO_2 and $Cu/ZnO/SiO_2$ catalysts was studied after reduction at 450–1300 K. The influence of the ZnO promoter on the exposed Cu surface area and metal cluster size was determined by N_2O chemisorption and X-ray diffraction. After reduction at 450 K, the metal surface area amounted to 9 m^2/gcat for both catalysts. Oxygen uptake during N_2O chemisorption increased significantly up to reduction temperatures of 800–900 K. This increase was most prominent for the ZnO-promoted catalyst, although no oxygen uptake was observed for a similarly treated ZnO/SiO_2 sample. The behaviour of the promoted catalyst can be explained by formation of Zn^0, surface alloying, and segregation of ZnO_x species on top of Cu clusters. The high thermostability of the catalysts was confirmed by *in situ* XRD measurements. The Cu crystallite size in both catalysts was about 4 nm, and did not increase when the reduction temperature was raised to 1100 K for 1 h.

2.1 Introduction

Contradictory views exist on the nature of active sites and the role of promoters in (supported) Cu/ZnO catalysts, which are widely used in the water gas shift reaction, ester hydrogenolysis, and both methanol synthesis and decomposition. Three main theories may be distinguished concerning the active state of copper in Cu/ZnO-based catalysts for methanol synthesis, *viz* Cu^0, Cu^{1+}, and a Cu/Zn alloy [1–3]. Depending on the gas phase and temperature, dynamic behaviour of the structure has been observed for which various models have been developed [4]: wetting/non-wetting phenomena of ZnO by

* E.D. Batyrev, J.C. van den Heuvel, J. Beckers, W.P.A. Jansen, and H.L. Castricum, *J. Catal.*, 2005, 229, 136.

metallic Cu [5], flat epitaxial Cu particles on top of ZnO balanced by dissolved protons [6], and coverage of Cu particles or mixed oxide by ZnO [7].

Brands *et al.* found that supported $Cu/ZnO/SiO_2$ catalysts reduced at high temperature exhibited a profound increase in the rate of methanol synthesis, as well as ester hydrogenolysis [8]. The conclusion from this and other works [9–11] is that the Cu–ZnO interface is crucial for the activation of carbonyl functions towards hydrogenation, possibly involving stabilisation of Cu^{1+} [4]. In a recent Low Energy Ion Scattering study, Jansen *et al.* reported that the surface composition of a similar $^{63}Cu/^{68}ZnO/SiO_2$ catalyst depends strongly on the applied reduction temperature [7]. Some ZnO enrichment of the surface was found after reduction at 473 K, while at 673 K virtually all Cu clusters were covered with partly reduced ZnO_x species ($0<x<1$). Consequently, the exposed Cu surface area is expected to be diminished due to shielding of metallic Cu by ZnO_x. This decrease was not observed by Brands *et al.*, who established a typical Cu surface area of 20 m^2/g_{cat} by N_2O chemisorption [8].

Although the catalytic activity of Cu/ZnO-based catalysts is found to correlate nicely with N_2O chemisorption data [12], Berndt *et al.* have shown that N_2O chemisorptions may overestimate the Cu surface area due to oxidation of partially reduced ZnO [13] and/or hydrogen dissolved in the ZnO matrix [14]. Contrarily, Jung *et al.* found that ZnO in the presence of Cu was not reduced by H_2 below 723 K [15]. Therefore, more information is needed on the question of how Cu/ZnO interaction at different reduction temperatures influences chemisorption by the $Cu/ZnO/SiO_2$ system. Since Brands *et al.* found a substantial rise in methanol synthesis activity with reduction temperature for ZnO-promoted catalysts and a modest methanol yield for Cu/SiO_2 catalysts [4, 16], a comparison between promoted and unpromoted catalysts is especially important.

In view of the above, the questions we want to address in this study concern (i) the structure of $Cu/ZnO/SiO_2$ catalysts, *i.e.*, the size and morphology of Cu nanoparticles and the nature of the Cu/ZnO interface, and (ii) the correctness of the N_2O chemisorption method to establish the Cu surface area. To these ends we applied TG and N_2O chemisorption combined with XRD and HR-TEM measurements on $Cu/ZnO/SiO_2$ and Cu/SiO_2 systems reduced in the temperature range of 450–1300 K, *i.e.*, well beyond the reduction temperature of 750 K established for maximal activity [8, 16]. Silica supported catalysts are well-suited to investigate Cu/ZnO interaction, because of the large surface area and the relatively mild chemical interaction with Cu and ZnO as compared to alumina. The loading of the support was chosen in conformity with the composition of the highly active catalyst for

ester hydrogenolysis and methanol synthesis investigated previously [11]. Moreover, the low Cu loading guarantees that sintering of the metal particles can be ruled out as much as possible.

2.2 Experimental

Promoted and unpromoted silica-supported copper catalysts were prepared by homogeneous deposition precipitation of copper nitrate trihydrate (Merck, > 99.5% pure) and zinc nitrate hexahydrate (Janssen, > 98% pure) onto Aerosil 200 silica (Degussa), according to the method described by Van der Grift *et al.* [17]. The precipitate was washed twice with doubly distilled water and dried at 363 K overnight. Subsequently, the precipitate was crushed and sieved to obtain the required size of the silica particles of 125–212 μm.

The metal loading of the prepared catalysts was determined by inductively coupled plasma atomic emission spectroscopy (ICP-AES) and amounted to Cu/SiO_2 (12.9 ± 0.5 wt% Cu) and $Cu/ZnO/SiO_2$ (12.9 ± 0.5 wt% Cu, 4.8 ± 0.2 wt% Zn).

XRD measurements were carried out by means of Cu-K_α radiation (λ = 0.154 nm) using a curved position-sensitive Philips CPS-120 diffractometer equipped with a high temperature reaction cell. This setup enabled *in situ* reduction of the catalysts in a 5% H_2/He flow at elevated temperatures up to 1300 K; the heating rate was 50 K/min. Samples were mounted on a Pt-plate with special glue. After background subtraction and correction for instrumental broadening, the peak width and diffraction angle 2θ were used to calculate the average crystallite size d [18]:

$$d = 0.94\lambda/(2\theta) \cdot \cos\theta$$

with λ the X-ray wavelength, and (2θ) the full width at half-maximum in radians. Transmission electron microscopy (TEM) and electron diffraction were performed using a Philips CM30UT electron microscope operated at 300 kV. In this microscope, energy dispersive X-ray (EDX) elemental analysis was carried out by means of a LINK EDX system.

Calcination, reduction and chemisorption of the catalysts were carried out in a Setaram TG-85 thermobalance to monitor the treatments; after each step the thermobalance was evacuated for 15 min. Samples of about 200 mg were placed into a porous basket and calcined in a flow of 2 cm^3/s dry air at 750 K for 12 h. Then the samples were heated in a flow of 2 cm^3/s 66% H_2/Ar with 72 K/h to the required reduction temperature, kept at this temperature for 1 h, and finally allowed to cool down to 363 K in the flowing reducing gas.

The sample weight during temperature programmed reduction was corrected for the changing gas density by subtracting the baseline obtained during the subsequent cool down. Differential thermogravimetric (DTG) profiles were calculated by differentiation of the corrected thermobalance data with time to include the 1 h hold-period; the obtained values are plotted against the temperature.

Copper surface areas were determined by N_2O chemisorptions [19], following the gravimetric method described by Luys *et al.* [20]. During dissociative chemisorption of N_2O by the catalyst, an oxidic layer is formed, according to the reaction

$$N_2O(g) + 2Cu^0_s \rightarrow (Cu–O–Cu)_s + N_2(g),$$

where Cu_s denotes a Cu surface site. Chemisorption was performed in a flow of 2 cm^3/s 1% N_2O/99 % Ar at 363 K during 50 min, and the amount of oxygen consumed was determined from the weight gain of the sample. The copper surface area was calculated by linear extrapolation of the subsurface contribution to $t = 0$ [20], assuming $Cu_s/O_{ads} = 2$, and a value of 1.46×10^{19} Cu_s atoms/m^2 for single crystal [21]. Since for the promoted catalyst partial reduction of ZnO is expected during high temperature reduction [13], oxygen uptake during N_2O chemisorption is expressed as 'metal surface area' in this study. The typical error in metal surface areas is about 5%. After chemisorption, the treated samples are denoted as passivated.

2.3 Results and discussion

2.3.1 X-ray diffraction

X-ray diffraction was employed to identify crystalline phases (Fig. 1) and to determine the crystallite size of supported particles (Fig. 2). The calcined samples show no sharp diffraction peaks, demonstrating that after calcinations the catalysts either have an amorphous structure or the size of the crystallites is smaller than the XRD detection limit. Subsequently, the calcined samples were reduced *in situ* at temperatures ranging from 500 to 1300 K.

The unpromoted Cu/SiO_2 catalyst reduced at 500 K exhibits two main peaks that can be assigned to Cu^0 (111) at $2\theta \approx 43.3^\circ$ and Cu^0 (200) at $2\theta \approx 50.5^\circ$ (Fig. 1a). The corresponding crystallite dimensions amount to *ca.* 4 and 3 nm, respectively (Fig. 2). Assuming the (111) plane parallel to the support [22], the slightly flattened particle shape would be indicative of a relatively weak interaction with the silica support. The Cu^0 peaks become more intense at reduction temperatures of 600–700 K when amorphous copper oxide is reduced quantitatively (see Section 3.3). From the stable crystallite

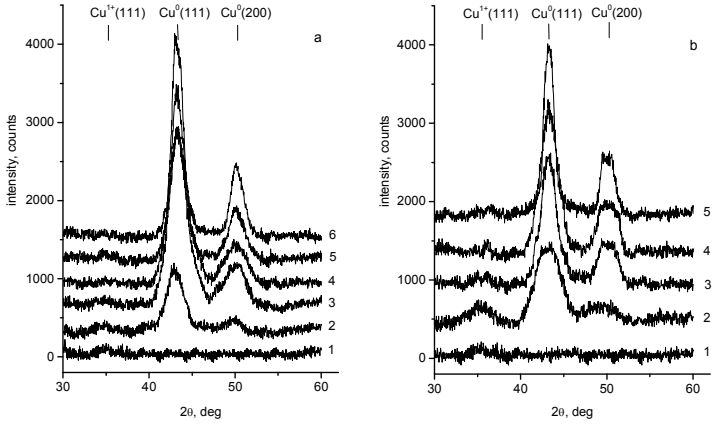

Fig. 1. (a) *X-ray diffraction patterns of the unpromoted Cu/SiO$_2$ catalyst after background subtraction. (1) Calcined; reduced at: (2) 500 K, (3) 600–900 K, (4) 1000 K, (5) 1200 K, and (6) 1300 K.*
(b) *X-ray diffraction patterns of the promoted Cu/ZnO/SiO$_2$ catalyst. (1) Calcined; reduced at: (2) 500 K, (3) 600–900 K, (4) 1000 K, and (5) 1300 K.*

size within a deviation of ±0.2 nm in the 600–1100 K range it may be inferred that sintering of the Cu particles can be excluded as well. Only after reduction at 1100 K the width of the Cu^0 peaks decreases, while the intensities become slightly higher. At the highest employed temperature of 1300 K, the calculated mean crystallite size amounts to *ca.* 6 nm. We conclude that for the unpromoted catalyst the Cu phase starts to grow by sintering of smaller crystallites after reduction at 1100 K.

The promoted Cu/ZnO/SiO$_2$ catalyst reduced at 500 K shows the same Cu^0 peaks, while no distinct crystalline ZnO phase (strongest line $2\theta \approx 36.2^\circ$) was observed (Fig. 1b). When the reduction temperature was raised to 600 K, the Cu crystallite size increased from 2.8 to 4.2 nm (Fig. 2), which may be related to partial crystallisation of amorphous Cu species. This finding is in good agreement with the dispersion ratio of 1.4 established by LEIS for the 473–573 K interval [7]. The size of the Cu crystallites up to reduction temperatures of 900 K appears rather constant (Fig. 2), the Cu^0 (111) plane being about 0.6 nm larger than the Cu^0 (200) plane. The digression encountered at 1000 K, which was found to be reproducible, is indicative of the formation of more spherical particles, and will be addressed in Section 2.3.5. Like the Cu/SiO$_2$ catalyst, the Cu crystallites of the promoted Cu/ZnO/SiO$_2$ catalyst were also found to grow at 1100 K.

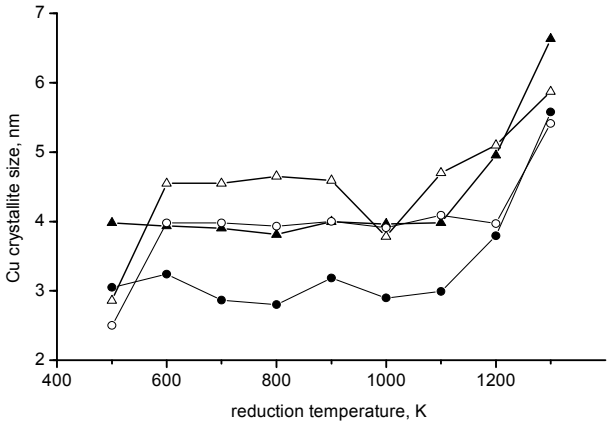

Fig. 2. *Size of Cu (111) and Cu (200) crystal planes from the XRD spectra of Cu/SiO_2 (solid symbols) and $Cu/ZnO/SiO_2$ (open symbols) catalysts at increasing reduction temperature. Assignment: triangles for Cu (111), circles for Cu (200).*

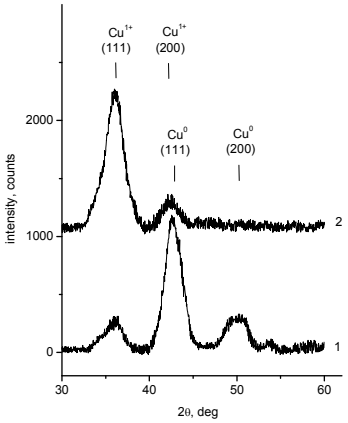

Fig. 3. *X-ray diffraction pattern after reduction at 800 K, N_2O passivation, and subsequent exposure to dry air at 363 K: (1) $Cu/ZnO/SiO_2$, (2) Cu/SiO_2.*

Following reduction at 800 K and passivation, Cu/SiO_2 and $Cu/ZnO/SiO_2$ catalysts were exposed to a flow of 2 cm^3/s dry air at 363 K in the thermobalance during 30 min. After 5 min of air

exposure, the weight of the Cu/SiO_2 sample reached a constant value that corresponded to the complete bulk oxidation of metallic Cu to Cu_2O. The XRD pattern of this oxidised sample only contained Cu^{1+} peaks of the (111) and (200) planes at $2\theta \approx 36.4^\circ$ and 42.3°, respectively (Fig. 3). Although not unexpected, it can be concluded that N_2O passivation does not protect Cu particles from further oxidation by air at 363 K.

Interestingly, a completely different result was obtained for the ZnO-promoted system. The passivated and aerated $Cu/ZnO/SiO_2$ sample still exhibited the familiar Cu^0 (111) and Cu^0 (200) peaks, while only a small Cu^{1+} (111) peak was obtained as compared to the unpromoted catalyst (Fig. 3). This strongly suggests that the majority of the metallic Cu particles in the ZnO-promoted catalyst was shielded from oxidation by air at 363 K. Most likely this arises from the coverage of Cu by ZnO_x species, as this substantially lowers the surface free energy of the system; see Table 1.

Table 1. *Surface free energy (γ) of metals [33] and oxides [34].*

	γ, mJ/m^2		γ, mJ/m^2
Zn	990	Cu	1825
ZnO	90	Cu_2O	825
SiO_2	605	CuO	530

2.3.2 Electron microscopy

High resolution electron microscopy images of catalysts reduced at 600–900 K were taken to visualise morphology, size and distribution of the supported Cu and ZnO phases. Although the EDX pattern of the $Cu/ZnO/SiO_2$ catalyst did contain a small Zn peak, no distinct ZnO particles could be distinguished on the micrographs. This finding confirms the amorphous character of the ZnO phase found with XRD.

The electron-dense Cu particles were seen in acceptable contrast with the silica support (see Fig. 4). Few Cu particles were clearly resolved and exhibited the proper d-spacing. Spherical Cu particles with a diameter of 3.9 ± 0.2 nm ($n = 144$) distributed evenly on the support were observed for both types of catalyst reduced in the range 600–900 K. By comparing the HR-TEM and XRD results it is concluded that the Cu particle and crystallite size are the same in the mentioned range of reduction temperatures, *i.e.*, the Cu phase is monocrystalline.

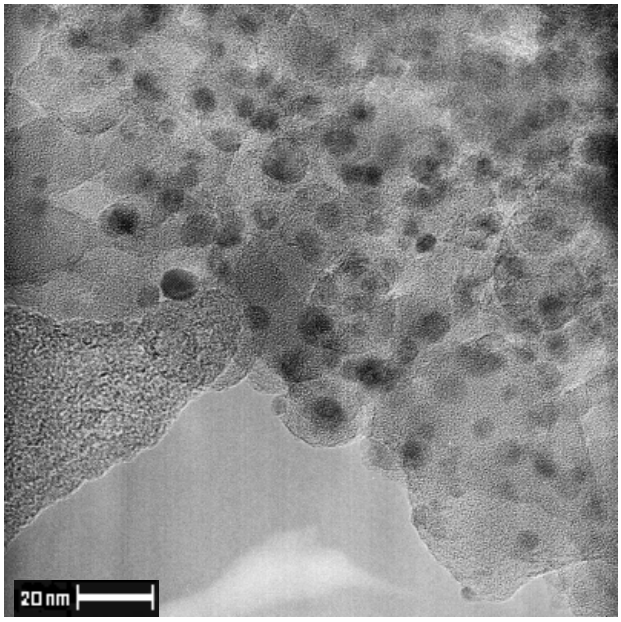

Fig. 4. *HR-TEM image of Cu/SiO_2 after reduction at 900 K.*

2.3.3 Thermogravimetry

DTG profiles were calculated to monitor the reduction process; as can be seen from Fig. 5 they exhibit very reproducible paths. The vertical lines at the end represent the weight loss during the hold-period when the final reduction temperature is reached. The unpromoted Cu/SiO_2 catalyst shows a sharp peak at 425 K, associated with the autocatalytic reduction of CuO clusters to Cu^0 [23]. The shoulder and tail at higher temperatures are usually assigned to the (stepwise) reduction of very small Cu particles that interact more strongly with the support [24, 25].

The main reduction peak of the promoted $Cu/ZnO/SiO_2$ catalyst is broader and found at a higher temperature of 450 K; this phenomenon is ascribed to interaction with ZnO, and has been reported to increase with the ZnO loading [11]. The pronounced tail is attributed to the progressive partial reduction of ZnO. Since the ZnO/SiO_2 reference does not consume any H_2 up to *ca.* 750 K, it is plausible that this tail can be assigned to a specific Cu/ZnO interaction. The huge and broad peak at $T_{red} > 800$ K is due to sublimation of the volatile Zn^0 from defective ZnO_x (see Section 2.3.5).

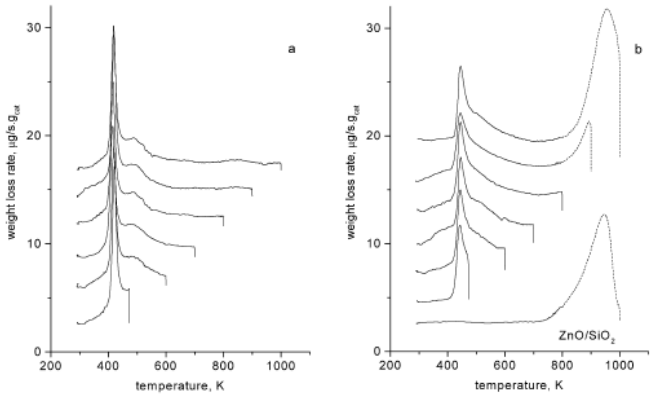

Fig. 5. *DTG profiles during reduction: (*a*) Cu/SiO₂, (*b*) Cu/ZnO/SiO₂ and ZnO/SiO₂ reference. Sublimation of Zn^0 is denoted by the dashed line.*

The total weight loss of the samples after reduction is plotted in Fig. 6, and also expressed as equivalent H_2 consumption per Cu atom. The reduction of the unpromoted Cu/SiO_2 catalyst is completed at 700 K when the H_2/Cu ratio equals 1; the further weight loss at T_{red} > 800 K may be attributed to either reduction or sintering of the silica support [26, 27]. The H_2 consumption of the promoted $Cu/ZnO/SiO_2$ catalyst exceeds 1 H_2/Cu atom at T_{red} = 600 K, and increases up to *ca.* 1.4 mol H_2/Cu atom at T_{red} = 800 K. The latter value corresponds to the H_2 consumption required to reduce all CuO and ZnO in the calcined catalyst. The dramatic weight loss at higher reduction temperatures is related to the above-mentioned sublimation of Zn^0 (see Section 2.3.5).

2.3.4 N_2O chemisorption

N_2O chemisorption measurements were performed on Cu/SiO_2 and $Cu/ZnO/SiO_2$ samples reduced at elevated temperatures. Highly reproducible results were obtained for both catalyst systems after successive reduction–passivation cycles. This is thought to indicate that the passivation treatment was mild enough not to result in significant structural changes. A ZnO/SiO_2 reference sample did not consume any oxygen from N_2O after reduction treatments at 500–1000 K. Consequently, no oxidisable Zn was formed in this sample.

For high-loaded Al_2O_3 supported systems it was reported that N_2O passivation induced modification of the Cu particle structure, ascribed to the heat of dissociative adsorption [28]; an H_2 TPD method was suggested by these authors to selectively measure the Cu

metal area. Here, values were found to be highly reproducible, which justifies the use of the direct method.

N_2O chemisorption curves exhibit two different slopes: a fast weight increase during the first 10 min attributed to surface oxidation, and a slow weight increase ascribed to subsurface oxidation that takes place simultaneously (Fig. 7) [20]. By increasing the N_2O concentration from 1 to 2%, the surface oxidation rate increased 1.6 times while the subsurface oxidation rate did not change. The zero order dependency of the latter was also reported by Luys *et al.* [20].

The corrected N_2O consumption, and thus the metal surface area, was not affected by doubling the nitrous oxide pressure. Therefore, it is concluded that mass transfer through the porous basket in the thermobalance was not limiting.

It should be noted that the subsurface oxidation rate increases with temperature [20]. Due to the heat of reaction, the local temperature during N_2O chemisorption will strongly depend on the size and roughness of the Cu particles, as well as on the thermal properties of the system. This implies that formation of 1 Cu_2O monolayer only, as found on large single crystal faces [29], is likely to be exceeded on the Cu nanoparticles of our supported catalyst.

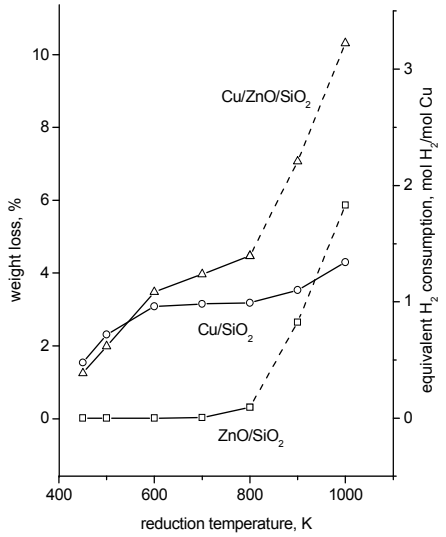

Fig. 6. *Weight loss after reduction and corresponding H_2 consumption per Cu atom of the ZnO-promoted catalyst (triangles) and unpromoted catalyst (circles) as a function of the reduction temperature. The weight loss after reduction of the ZnO/SiO_2 reference is also included (squares); sublimation of Zn^0 is denoted by dashed lines.*

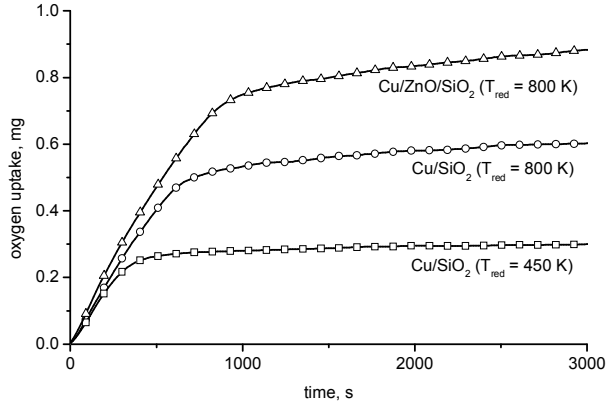

Fig. 7. *Oxygen uptake during N_2O chemisorption for supported Cu catalysts.*

Initially, a substantial increase in oxygen uptake with reduction temperature is obtained for both Cu/SiO_2 and $Cu/ZnO/SiO_2$ systems (Figs. 7 and 8). The behaviour of the unpromoted system can be explained by the increasing reduction degree of the copper particles at higher temperatures (see Fig. 6). The Cu surface area for this system has a maximum value of 16 m^2/g_{cat} at 900 K (Fig. 8).

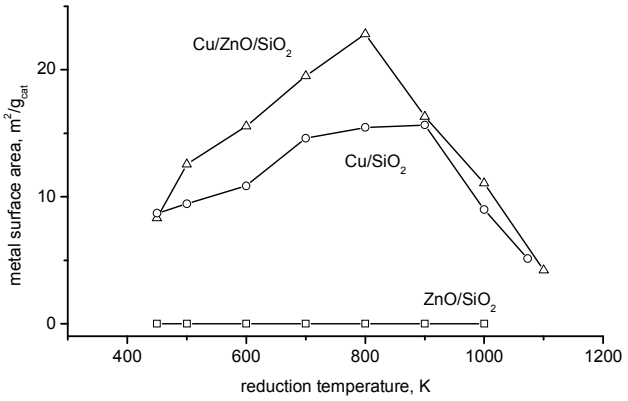

Fig. 8. *Equivalent metal surface area of the ZnO-promoted catalyst (triangles) and unpromoted catalyst (circles) as a function of the reduction temperature. The ZnO/SiO_2 reference is also included (squares).*

After reduction at higher temperatures the Cu surface area dramatically decreased to 5 m^2/g_{cat} at 1073 K, although the XRD results indicate that sintering of Cu crystallites does not occur below 1100 K. The difference can be explained when it is assumed that after reduction above 900 K part of the Cu clusters is encapsulated by silica, driven by reduction of the surface free energy (see Table 1). It is known that silica sinters at high temperatures, which is accompanied and impelled by condensation of surface Si–OH groups [27, 30]; the associated weight decrease was also indicated by the TG data at $T_{red} > 800$ K.

After reduction at 450 K the same metal surface area was obtained for the ZnO-promoted and unpromoted catalyst, indicating equally sized Cu clusters. However, the metal surface area of the promoted system increases much stronger to reach a maximum value of 23 m^2/g_{cat} after reduction at 800 K (Fig. 8). Based on the smallest particle size of 4 nm obtained from XRD, a maximal Cu surface area of 19 m^2/g_{cat} can be calculated for the fully reduced $Cu/ZnO/SiO_2$ catalyst. The extra N_2O consumption plus the weight loss during reduction in excess of the Cu-stoichiometry provide strong arguments that partially reduced ZnO_x species are formed in the presence of Cu, and that the interaction between Cu and ZnO increases with reduction temperature. Considering the observed shielding of Cu crystallites in the promoted system from oxidation by air, it is tentatively concluded that a partially reduced ZnO_x layer is formed on top of the metallic Cu phase.

It should be noted that metallic Zn requires twice as much oxygen as Cu upon oxidation by N_2O. Furthermore, the *ca.* 15% faster surface oxidation rate of the promoted catalyst after reduction at 800 K (see Fig. 7) can be explained by the higher affinity of Zn for oxidation compared to Cu [31].

A further increase of the reduction temperature to 900 K led to a decreasing metal surface area of the $Cu/ZnO/SiO_2$ catalyst (Fig. 8). ICP-AES analysis revealed that this can be attributed to sublimation of metallic Zn from the partially reduced ZnO_x species (see Section 2.3.5). Interestingly, removal of the ZnO_x layer from the Cu clusters leads to the exposure of almost the same metal surface area as in case of the unpromoted catalyst reduced at 900 K. It should be stressed that XRD measurements had already proven that the size of Cu crystallites in the promoted catalyst remained unchanged up to 900 K, excluding sintering as the cause of the decreased metal surface area.

2.3.5 ICP-AES analysis

The origin of the large weight losses of the promoted catalyst during reduction at high temperatures was identified using ICP-AES analysis. The metal content of the $Cu/ZnO/SiO_2$ catalyst and ZnO/SiO_2 reference after reduction at 300–1000 K are presented in Table 2 and expressed as residue compared to the freshly prepared material. While no ZnO is lost during calcination at 750 K (results not shown), it is obvious that the separate ZnO phase from the reference starts to disappear when heated above 800 K in a reducing atmosphere. This is thought to occur by the creation of oxygen vacancies and subsequent sublimation of highly volatile Zn^0. At 1000 K all Zn has vanished from the reference system. In contrast, Zn from the promoted catalyst is more stable with a 12% residue persisting up to 1000 K.

Table 2. *Cu and Zn residue of the $Cu/ZnO/SiO_2$ catalyst and the ZnO/SiO_2 reference system after reduction at different temperatures T_{red}, as obtained from ICP-AES analysis.* ND: *not detectable*

T_{red}, K	$Cu/ZnO/SiO_2$		ZnO/SiO_2
	Cu_{red}/Cu_{fresh}	Zn_{red}/Zn_{fresh}	Zn_{red}/Zn_{fresh}
300	1.00	1.00	1.00
700	1.01	1.01	1.01
800	1.02	1.02	0.95
900	1.00	0.66	0.55
1000	1.02	0.12	ND

Interestingly, the Zn residue of the $Cu/ZnO/SiO_2$ catalyst after reduction at 900 K is also some 12% higher than the reference. This quantitative concurrence is thought to indicate brass formation, which is also required for thermodynamic reasons to reduce ZnO with H_2 [15]. It can be calculated that Cu particles with an average size of 4.0 nm, as found with XRD, require 60% of the total Zn amount to be covered completely with 1 monolayer of metallic Zn. So it may be speculated that 12%/60% = 0.2 monolayer of metallic Zn is present as a stable $Cu_{0.8}Zn_{0.2}$ surface alloy covering the Cu particles. Alloy formation has been suggested to occur under severe reducing conditions by various authors, e.g., [3, 30, 32]. Unlike a ZnO_x layer covering metallic Cu, it seems that such a surface alloy does not bring about additional N_2O consumption during passivation (see Fig. 8).

Since the disappearance of the covering ZnO_x layer around 900 K will lead to an increased surface tension of the Cu clusters, the sudden decrease of the Cu(111) plane at 1000 K (see Fig. 2) may be explained by formation of more spherical Cu particles.

2.4 Comparison with LEIS results

LEIS studies on $^{63}Cu/^{68}ZnO/SiO_2$ catalysts by Jansen *et al.* [7] have established that the composition of the outermost layer depends strongly on the applied reduction temperature. In the range 473–673 K the CuO_x surface atomic density decreased from 4.4 to 0.1%, while that of ZnO_x remained *ca.* 4%. These dispersion data can be explained by some sintering of highly dispersed Cu particles until a 'final' size of 4 nm, followed by their complete coverage with ZnO_x at higher reduction temperatures. The quantitative use of ZnO to cover the Cu clusters provides maximal metal–promoter interaction, which might explain the optimal Zn content of *ca.* 5 wt% found for this catalyst for ester hydrogenolysis and methanol synthesis [11].

Depth profiles showed a rapid decrease of the Zn concentration with the ion dose, indicating that the enriched layer has a thickness of 1–2 monolayers only. From the 4.8 wt% Zn loading and the reported BET surface area of this catalyst of 350 m^2/g [11] it can be calculated that 2.6 ZnO monolayers would be needed to obtain the experimental surface atomic density, *i.e.*, cluster surface area of 4%.

The oxidation state of the Cu and Zn atoms at the catalyst surface was established by comparing the LEIS signals before and after N_2O passivation. After reduction at 473 K the atomic composition of the outermost cluster surface was 42% Zn^{2+}, 2%Zn^0, 54% Cu^{1+}, and 2% Cu^0 [7]. This means that 96% of the outermost Cu surface was oxidic in nature, although we know from TG data that *ca.* 60% of the CuO bulk has been reduced at 473 K (see Fig. 6). This outer Cu^{1+} layer serves the purpose of reducing the surface free energy (see Table 1), but its presence in the reduced state implies that N_2O chemisorption readily affects oxidation of at least 1 subsurface layer. It should be noted that the distinction between surface and subsurface oxidation according to Luys *et al.* [20] is purely based on kinetics (see also Fig. 7).

After reduction at 673 K the atomic composition of the outermost cluster surface was 77% Zn^{2+}, 19% Zn^0, 3% Cu^{1+}, and 1% Cu^0 [7], which clearly illustrates coverage of the Cu particles by Zn as well as reduction of ZnO in close contact with Cu. About two ZnO_x layers of this composition - with a Zn^0 fraction of 20% of the total Zn - would be needed to account for the oxygen uptake during passivation, which corresponds to 22% of the total Zn amount.

It is concluded that the general behaviour of the $Cu/ZnO/SiO_2$ catalyst deduced from the present XRD, N_2O chemisorption, and ICP-AES data, is in good agreement with the results obtained previously with LEIS. A quantitative correspondence

of the N_2O chemisorption data requires fast oxidation of Cu^0 and Zn^0 in 1–2 additional layers at T_{red} = 473 and 673 K, respectively.

2.5 Conclusions

XRD, TG, N_2O chemisorption, and ICP-AES characterisation of Cu/SiO_2 and $Cu/ZnO/SiO_2$ catalysts reduced at 450–1300 K enabled to study the behaviour of the different phases. The present results are consistent with those obtained with LEIS, and allow a better understanding of the structure of the highly active $Cu/ZnO/SiO_2$ catalyst reduced at 750 K.

Cu/ZnO interaction is responsible for the formation of special sites consisting of 4 nm Cu crystallites covered by 1–2 monolayers of partially reduced ZnO_x species. Formation of those sites starts after reduction at 450 K and increases up to 800 K. Reduction in the range 800–900 K leads to sublimation of the covering ZnO_x layer, thereby exposing the original Cu crystallites that probably have undergone surface alloying at some stage of the treatment. At reduction temperatures > 900 K, the Cu particles are likely to be encapsulated by the supporting SiO_2. At still higher reduction temperatures the Cu crystallites start to sinter. Nevertheless, these SiO_2 supported systems can be considered as highly thermostable.

The dynamic structure of this methanol synthesis catalyst can be explained well by minimisation of the surface free energy of the Cu clusters. Reduction of the smallest CuO crystallites is completed only at 700 K, while the 4 nm Cu particles are fully covered with partially reduced ZnO_x species that protect metallic Cu largely from oxidation by air. At the same time, the Cu/ZnO interface is maximised, and it seems that no separate ZnO phase is present in catalysts of this composition. After sublimation of ZnO_x at very high reduction temperatures, the surface free energy of the system is lowered by encapsulation, and finally by sintering of the Cu particles.

Within the range 450–800 K, the amorphous ZnO phase was partially reduced only in the presence of Cu, which might be explained by surface alloying. This is supported further by the fact that metallic Zn in defective ZnO_x on top of Cu is oxidised reversibly by N_2O chemisorption. As a consequence, this method overestimates the Cu surface area of $Cu/ZnO/SiO_2$ catalysts. Otherwise, N_2O passivation of Cu nanoparticles does not saturate at the formation of a single Cu_2O layer.

Acknowledgments

Dr. P.J. Kooyman (Delft University of Technology, The Netherlands) is acknowledged for performing electron microscopy investigations. The Netherlands Organisation for Scientific Research STW/NWO, Shell Global Solutions, and Johnson Matthey Catalysts, are gratefully acknowledged for financial support.

References

1. G.C. Chinchen, K.C.Waugh, and D.A.Whan, *Appl. Catal.*, 1986, 25, 101.
2. K. Klier, *Adv. Catal.*, 1982, 31, 243.
3. J. Nakamura, Y. Choi, and T. Fujitani, *Top. Catal.*, 2003, 22, 277.
4. E.K. Poels and D.S. Brands, *Appl. Catal. A*, 2000, 191, 83.
5. B.S. Clausen, J. Schiøtz, L. Gråbæk, C.V. Ovesen, K.W. Jacobsen, J.K. Nørskov, and H. Topsøe, *Top. Catal.*, 1994, 1, 367.
6. T. Yurieva, L.M. Plyasova, O.V.Makarova, and T.A. Krieger, *J.Mol. Catal. A*, 1996, 113, 455.
7. W.P.A. Jansen, J. Beckers, J.C. van den Heuvel, A.W. Denier van der Gon, A. Bliek, and H.H. Brongersma, *J. Catal.*, 2002, 210, 229.
8. D.S. Brands, E.K. Poels, T.A. Krieger, O.V. Makarova, C. Weber, S. Veer, and A. Bliek, *Catal. Lett.*, 1995, 36, 175.
9. J. Nakamura, I. Nakamura, T. Uchijima, Y. Kanai, T. Watanabe, M. Saito, and T. Fujitani, *Catal. Lett.*, 1995, 31, 325.
10. J.E. Bailie, C.H. Rochester, and G.J. Millar, *Catal. Lett.*, 1995, 31, 333.
11. F.T. van de Scheur and L.H. Staal, *Appl. Catal. A*, 1994, 108, 63.
12. H.L. Castricum, H. Bakker, B.v.d. Linden, and E.K. Poels, *J. Phys. Chem. B*, 2001, 105, 7928.
13. H. Berndt, V. Briehn, and S. Evert, *Appl. Catal. A*, 1992, 86, 65.
14. H. Berndt, V. Briehn, and S. Evert, *J. Mol. Catal.*, 1992, 73, 203.
15. K.D. Jung, O.S. Joo, and S.H. Han, *Catal. Lett.*, 2000, 68, 49.
16. D.S. Brands, *PhD thesis, University of Amsterdam*, 1998.
17. C.J.G. van der Grift, P.A. Elberse, A. Mulder, and J.W. Geus, *Appl. Catal.*, 1990, 59, 275.
18. B.E. Warren, *X-ray Diffraction, Addison–Wesley, Reading, MA*, 1980.
19. G.C. Chinchen, C.M. Hay, H.D. Vandervell, and K.C.Waugh, *J. Catal.*, 1987, 103, 79.
20. M.J. Luys, P.H. van Oefelt, W.G.J. Brouwer, A.P. Pijpers, and J.F.F. Scholten, *Appl. Catal.*, 1989, 46, 161.
21. J.W. Evans, M.S. Wainwright, A.J. Bridgewater, D.J. Young, *Appl. Catal.*, 1983, 7, 75.

22. P.L. Hansen, J.B. Wagner, S. Helveg, J.R. Rostrup-Nielsen, B.S. Clausen, and H. Topsøe, *Science*, 2002, 295, 2054.
23. M.J. Tiernan, P.A. Barnes, and G.M.B. Parkes, *J. Phys. Chem. B*, 1999,103, 338.
24. M. Shimokawabe, N. Takezawa, and H. Kobayashi, *Bull. Chem. Soc. Jpn.*, 1983, 56, 1337.
25. E.D. Guerreiro, O.F. Gorriz, J.B. Rivarola, and L.A. Arrúa, *Appl. Catal. A*, 1997, 165, 259.
26. M. Komiyama, and T. Shimaguchi, *Surf. Interface Anal.*, 2001, 32, 189.
27. R.K. Iler, *The Chemistry of Silica, Wiley, New York,* 1979.
28. M. Muhler, L.P. Nielsen, E. Törnqvist, B.S. Clausen, and H. Topsøe, *Catal. Lett.*, 1992, 14, 241.
29. F.H.P.M. Habraken, C.M.A.M. Mesters, and G.A. Bootsma, *Surf. Sci.*, 1980, 97, 264.
30. N.-Y. Topsøe and H. Topsøe, *J. Mol. Catal. A*, 1999, 141, 95.
31. K.L. Siefering and G.L. Griffin, *Surf. Sci.*, 1989, 207, 525.
32. J.-D. Grunwaldt, A.M. Molenbroek, N.-Y. Topsøe, H. Topsøe, and B.S. Clausen, *J. Catal.*, 2000, 194, 452.
33. F.R. de Boer, R. Boom, W.C.M. Mattens, A.R. Miedema, and A.K. Niessen, *Cohesion in Metals, North-Holland, Amsterdam*, 1988.
34. S.H. Overbury, P.A. Bertrand, and G.A. Somorjai, *Chem. Rev.,* 1975, 75, 547.